

Thermomechanical Models of Air Gap Nucleation During Pure Metal Solidification on Moving Molds with Periodic Surface Topographies

Louis G. Hector, Jr.
Surface Science Division, Alcoa
Industry Representative

Michael Booty, New Jersey Institute of Technology
Michelle DeBonis, New Jersey Institute of Technology
David A. Edwards, University of Delaware
Donald A. French, University of Cincinnati
Alistair Fitt, University of Southampton
Peter Howell, University of Oxford
John King, University of Nottingham
John Pelesko, California Institute of Technology
and others...

Fourteenth Annual Workshop on Mathematical Problems in Industry
June 8–12, 1998
Rensselaer Polytechnic Institute

Section 1: Introduction

The occurrence of air gaps at the interface between a forming mold and the solidifying melt it contains is regarded as a serious problem in the metal castings industry. When surface air gaps form or *nucleate*, heat transfer between the part of the melt that has already solidified and the mold decreases locally, introducing a source of nonuniformity and temperature gradients tangential to the mold surface. Transverse temperature gradients induce irregularities in the solidification front that propagate through the melt and differential thermomechanical stresses in the solidified part of the melt. Since stresses in the solidified melt may themselves be the cause of air gaps forming at the mold surface, the sequence of cause and effect in the formation of air gaps is not clear. However, the result is, in progressively worse cases, irregularities in the casting, followed by interior cracks, and, ultimately, a weakening and failure of the casting in use. It has been suggested that air gap nucleation and spatial variation in the heat extraction profile at the mold-melt interface may be caused by irregularities in the mold surface due to effects such as mold topography, the use of separating agents, or the presence of oxides.

The problem brought to the Mathematical Problems in Industry (MPI) workshop by Louis G. Hector Jr. (Surface Science Division, Alcoa Technical Center) was to derive and solve a mathematical model for the thermomechanical behavior of the casting process. The model is based on a series of experiments in which a cold metal cube or block, insulated on all sides except for one bare vertical side, is immersed at constant speed into a bath of aluminum that is initially just above its melting temperature. A wedge-shaped sample of solidified aluminum forms on the cold, bare, vertical ‘mold’ surface. The sample is widest near its lowest point, where the time over which solidification has occurred is greatest, and has zero width at the point where the mold enters the bath. The experiment is stopped instantaneously, and the shape of the wedge surface, which can be ‘wavy’, indicates the evolution in time of a solidification front as it propagates through a casting.

The specific goal was to derive expressions for the contact pressure at the mold-melt interface, including the case of purely sinusoidal variations imposed on the mold surface topography. It was expected that, among other things, expressions for the contact pressure would depend on the wavelength of the mold topography; see [1] for more discussion and further references. Air gaps are assumed to form at points where the contact pressure is zero.

In this report we describe work done on the problem during the week of the workshop. The first task was a derivation of dimensionless governing equations and boundary conditions to describe both heat transfer and elasticity effects in the solidified melt. The two effects are coupled as follows:

1. The boundary condition describing heat transfer at the mold-cast interface is such that the heat flux leaving the solid melt is proportional to the difference in temperature between the solid melt and the mold, where the constant of proportionality is a (known) function of the contact pressure. This is the coupling from the elastic field

to the thermal field.

2. The temperature appears in the diagonal components of the stress tensor for elastic stresses in the solidified melt as a result of thermal expansion and contraction. This is the coupling from the thermal to the elastic field.

We scaled the governing system and estimated the resulting scaling parameters based on experimental data. Approximate (asymptotic) solutions were found for the thermal field. The system decouples since the dependence of solid temperature on contact pressure appears only parametrically *via* the contact resistance in the boundary condition at the mold-melt interface. Next, the stress field in the solidified melt was incorporated, leading to a nonlinear ordinary differential equation describing the solidification front that propagates through the melt. Lastly, we investigated the effect of small-amplitude sinusoidal variations in mold surface topography on the thermal field.

We now outline the contents of the report. In §§2–5 we study the Stefan problem appropriate for heat conduction in the solidifying melt. The dimensionless Stefan problem is given in §2. A small parameter ϵ is identified, equal to the length scale x_c of temperature variation due to heat transfer from the solidified melt to the mold divided by a length scale z_c associated with the speed of propagation of the solidification front in the melt.

In §§3 and 4 two approximate solutions to the Stefan problem are found in the limit of small ϵ . In the first of these, the Stefan number St , defined as the ratio of sensible to latent heat, is also assumed to be small. Furthermore, we construct explicit results for the temperature field and solidification front position near the tip. In §4 we use approximate methods (see [2]) to obtain the initial development of the solidification front at moderate values of the Stefan number, which is estimated to be around 5 in the experiment under consideration. The resulting analysis leads to approximate solutions, as series expansions in ϵ , for the temperature in the solidified melt in terms of the location of the solidification front and the contact resistance. The position of the solidification front is described by a first order differential equation.

In §5 we consider the influence of small-amplitude undulations imposed on the mold surface. The undulations are considered to be in the direction parallel to the mold motion. The wavelength of this mold topography is assumed to be $O(x_c)$, and is thus much less than the original length scale z_c in the direction tangential to the mold. The method of multiple scales [3] is applied to determine the form of undulations induced in the solidification front in terms of the contact resistance. We also derive equations for the dynamics near the tip, where we expect the effects of the undulations to be most pronounced.

In §6 we study deformation of the solidified melt caused by thermal contraction during solidification and cooling. Of primary interest is a derivation of the contact pressure p on the mold-cast interface. The governing equations of linear hypo-thermo-elasticity are used, and stresses are written in terms of the Airy stress function (or potential). Terms in the equations at $O(\epsilon)$ are discarded to compute a leading-order expression for the contact pressure as a function of temperature in the solidified melt. The results of §3 are then used to find the contact pressure in terms of the location of the solidification front; the pressure is then eliminated to find a nonlinear, third-order differential equation for the location of the solidification front alone.

Section 2: Governing Equations

We wish to model the immersion of a metal mold into a bath of molten metal maintained at a constant freezing temperature T_f (see Fig. 1). The mold moves with velocity V in the \tilde{z} -direction. All sides of the mold, save one, are insulated. The remaining face ($\tilde{x} = \tilde{x}_s$) is exposed to the melt and the molten metal begins to solidify there.

We idealize this problem using a mold which is infinite in two directions and semi-infinite in the third (\tilde{x} , see Fig. 2). The surface of the mold may have an irregular shape and vary in time due to the motion in the \tilde{z} -direction, so we define the mold boundary to be $\tilde{x} = \tilde{x}_s(\tilde{z}, \tilde{t})$. The molten metal will begin to solidify against the cool surface of the mold in the \tilde{x} -direction. (The problem is uniform in the third direction.) Hence, there will be a moving solidification front $\tilde{x} = \tilde{s}(\tilde{z}, \tilde{t})$ between the solid and the molten liquid. For the solid region, the governing equation is the following convection-diffusion equation:

$$\rho c_p \left(\frac{\partial \tilde{T}}{\partial \tilde{t}} + V \frac{\partial \tilde{T}}{\partial \tilde{z}} \right) = k \left(\frac{\partial^2 \tilde{T}}{\partial \tilde{x}^2} + \frac{\partial^2 \tilde{T}}{\partial \tilde{z}^2} \right), \quad \tilde{x}_s(\tilde{z}, \tilde{t}) \leq \tilde{x} \leq \tilde{s}(\tilde{z}, \tilde{t}), \quad (2.1)$$

where ρ is the density, c_p is the specific heat, \tilde{T} is the temperature, and k is the thermal conductivity of the solid.

At the surface of the mold we impose the heat flux using Newton's Law of Cooling. Since the surface of the mold is maintained at room temperature, this condition may be written as

$$k \left[1 + \left(\frac{\partial \tilde{x}_s}{\partial \tilde{z}} \right)^2 \right]^{-1/2} \left(\frac{\partial \tilde{T}}{\partial \tilde{x}} - \frac{\partial \tilde{x}_s}{\partial \tilde{z}} \frac{\partial \tilde{T}}{\partial \tilde{z}} \right) (\tilde{x}_s(\tilde{z}, \tilde{t}), \tilde{z}, \tilde{t}) = \frac{\tilde{T}(\tilde{x}_s(\tilde{z}, \tilde{t})) - T_s}{\tilde{R}(\tilde{z}, \tilde{t})}, \quad (2.2)$$

where T_s is room temperature and \tilde{R} is the thermal contact resistance. (It will depend on \tilde{z} and \tilde{t} through the contact pressure \tilde{p} .) The left-hand side results from writing down the flux in the direction normal to the front.

At the solid-fluid interface, we must impose two conditions. First, the temperature has been specified at the freezing temperature T_f :

$$\tilde{T}(\tilde{s}(\tilde{z}, \tilde{t}), \tilde{z}, \tilde{t}) = T_f. \quad (2.3)$$

In addition, we specify the standard Stefan condition at the solid-liquid interface. In other words, the flux normal to the interface is proportional to the normal velocity of the front:

$$k \left(\frac{\partial \tilde{T}}{\partial \tilde{x}} - \frac{\partial \tilde{s}}{\partial \tilde{z}} \frac{\partial \tilde{T}}{\partial \tilde{z}} \right) (\tilde{s}(\tilde{z}, \tilde{t}), \tilde{z}, \tilde{t}) = \rho L \left(\frac{\partial \tilde{s}}{\partial \tilde{t}} + V \frac{\partial \tilde{s}}{\partial \tilde{z}} \right), \quad (2.4)$$

where L is the latent heat of fusion of the aluminum. The second term on the right arises from the fact that there is a contribution to the front motion from the motion of the mold itself.

To normalize the problem, we introduce the following scalings:

$$T(x, z, t) = \frac{\tilde{T}(\tilde{x}, \tilde{z}, \tilde{t}) - T_s}{T_f - T_s} = \frac{\tilde{T}(\tilde{x}, \tilde{z}, \tilde{t}) - T_s}{\Delta T}, \quad \Delta T = T_f - T_s, \quad s(z, t) = \frac{\tilde{s}(\tilde{z}, \tilde{t})}{x_c}, \quad (2.5a)$$

$$R(z, t) = h\tilde{R}(\tilde{z}, \tilde{t}), \quad x = \frac{\tilde{x}}{x_c}, \quad z = \frac{\tilde{z}}{z_c}, \quad t = \frac{\tilde{t}}{t_c}, \quad (2.5b)$$

where h is the heat transfer coefficient at hydrostatic pressure. To obtain x_c , we use the Neumann condition at $\tilde{x} = 0$. Substituting (2.5) into (2.2), we have

$$\left[1 + \frac{x_c^2}{z_c^2} \left(\frac{\partial x_s}{\partial z} \right)^2 \right]^{-1/2} k \Delta T \left(\frac{1}{x_c} \frac{\partial T}{\partial x} - \frac{x_c}{z_c^2} \frac{\partial x_s}{\partial z} \frac{\partial T}{\partial z} \right) (x_s(z, t), z, t) = \frac{h(\Delta T)T(x_s(z, t), z, t)}{R(z, t)}$$

$$\frac{k}{h} \left[1 + \epsilon^2 \left(\frac{\partial x_s}{\partial z} \right)^2 \right]^{-1/2} \left(\frac{\partial T}{\partial x} - \epsilon^2 \frac{\partial x_s}{\partial z} \frac{\partial T}{\partial z} \right) (x_s(z, t), z, t) = \frac{x_c T(x_s(z, t), z, t)}{R(z, t)}, \quad (2.6a)$$

$$\epsilon = \frac{x_c}{z_c}, \quad (2.6b)$$

where we expect $0 < \epsilon \ll 1$. To obtain an $O(1)$ heat flux we set

$$x_c = \frac{k}{h}, \quad (2.7a)$$

which is equivalent to setting the Biot number equal to 1 at hydrostatic pressure. Thus (2.6a) becomes

$$\left[1 + \epsilon^2 \left(\frac{\partial x_s}{\partial z} \right)^2 \right]^{-1/2} \left(\frac{\partial T}{\partial x} - \epsilon^2 \frac{\partial x_s}{\partial z} \frac{\partial T}{\partial z} \right) (x_s(z, t), z, t) = \frac{T(x_s(z, t), z, t)}{R(z, t)}. \quad (2.7b)$$

Substituting (2.5) and (2.7a) into (2.4), we have

$$k \Delta T \left(\frac{1}{x_c} \frac{\partial T}{\partial x} - \frac{x_c}{z_c^2} \frac{\partial s}{\partial z} \frac{\partial T}{\partial z} \right) (s(z, t), z, t) = \rho L x_c \left(\frac{1}{t_c} \frac{\partial s}{\partial t} + \frac{V}{z_c} \frac{\partial s}{\partial z} \right),$$

$$\left(\frac{\partial T}{\partial x} - \epsilon^2 \frac{\partial s}{\partial z} \frac{\partial T}{\partial z} \right) (s(z, t), z, t) = \frac{\rho L x_c^2}{k \Delta T t_c} \left(\frac{\partial s}{\partial t} + \frac{V t_c}{z_c} \frac{\partial s}{\partial z} \right). \quad (2.8)$$

To balance front motion with the flux term, we set

$$t_c = \frac{\rho L x_c^2}{k \Delta T} = \frac{\rho L k}{h^2 \Delta T}. \quad (2.9a)$$

To balance the effects of convection and unsteady flow, we set

$$z_c = Vt_c = \frac{\rho L k V}{h^2 \Delta T} \quad \implies \quad \epsilon = \frac{h \Delta T}{\rho L V}. \quad (2.9b)$$

Making these substitutions into (2.8), we obtain

$$\left(\frac{\partial T}{\partial x} - \epsilon^2 \frac{\partial s}{\partial z} \frac{\partial T}{\partial z} \right) (s(z, t), z, t) = \frac{\partial s}{\partial t} + \frac{\partial s}{\partial z}. \quad (2.10)$$

In addition, equation (2.3) becomes

$$T(s(z, t), z, t) = 1. \quad (2.11)$$

Substituting (2.5), (2.7a), and (2.9) into (2.1), we obtain the following:

$$\begin{aligned} \rho c_p \Delta T \left(\frac{1}{t_c} \frac{\partial T}{\partial t} + \frac{V}{z_c} \frac{\partial T}{\partial z} \right) &= k \Delta T \left(\frac{1}{x_c^2} \frac{\partial^2 T}{\partial x^2} + \frac{1}{z_c^2} \frac{\partial^2 T}{\partial z^2} \right), \quad 0 \leq x \leq s(x, t) \\ \rho c_p \frac{h^2 \Delta T}{k \rho L} \left(\frac{\partial T}{\partial t} + \frac{\partial T}{\partial z} \right) &= k \frac{h^2}{k^2} \left(\frac{\partial^2 T}{\partial x^2} + \epsilon^2 \frac{\partial^2 T}{\partial z^2} \right), \\ \text{St} \left(\frac{\partial T}{\partial t} + \frac{\partial T}{\partial z} \right) &= \frac{\partial^2 T}{\partial x^2} + \epsilon^2 \frac{\partial^2 T}{\partial z^2}, \quad \text{St} = \frac{c_p \Delta T}{L}. \end{aligned} \quad (2.12)$$

Here St is the *Stefan number*.

Using the values from the Appendix, we have

$$t_c = 4.18 \text{ s}, \quad (2.13a)$$

$$z_c = 0.42 \text{ m}, \quad (2.13b)$$

$$x_c = 2.4 \times 10^{-2} \text{ m}, \quad (2.13c)$$

$$\epsilon = 5.81 \times 10^{-2}, \quad (2.13d)$$

$$\text{St} = 4.88. \quad (2.13e)$$

Therefore, we see that $0 < \epsilon \ll 1$, as surmised.

Section 3: Flat Surface, Small St

We now tackle the equations arising from the problem of a flat mold plunging into the molten metal. In this case, we have that

$$x_s(z, t) = 0,$$

so equation (2.7b) becomes

$$\frac{\partial T}{\partial x}(0, z, t) = \frac{T(0, z, t)}{R(z, t)}. \quad (3.1)$$

We begin by considering the case of small St. This contradicts (2.13e), but we note that since c_p appears nowhere else in our problem, we can run an experiment with a different material to validate the theory. In addition, we shall show that in the limit of small z , the small St and moderate St limits for the front position are the same.

Letting St be our perturbation parameter, we have

$$T(x, z, t; \text{St}) \sim T_0(x, z, t) + \text{St}T_1(x, z, t) + o(\text{St}), \quad s(z, t; \text{St}) \sim s_0(z, t) + \text{St}s_1(z, t) + o(\text{St}). \quad (3.2)$$

For now, we do not expand R in a series in St. We wish to neglect the ϵ^2 terms in our equations, and hence we choose $\epsilon = o(\text{St}^{1/2})$. Substituting these expressions into (2.12), (3.1), (2.10), and (2.11), we obtain, to leading orders,

$$\text{St} \left[\frac{\partial(T_0 + \text{St}T_1)}{\partial t} + \frac{\partial(T_0 + \text{St}T_1)}{\partial z} \right] = \frac{\partial^2(T_0 + \text{St}T_1)}{\partial x^2} + \epsilon^2 \frac{\partial^2(T_0 + \text{St}T_1)}{\partial z^2} \quad (3.3a)$$

$$\frac{\partial^2 T_0}{\partial x^2} = 0, \quad (3.3a)$$

$$\frac{\partial^2 T_1}{\partial x^2} = \frac{\partial T_0}{\partial t} + \frac{\partial T_0}{\partial z}, \quad (3.3b)$$

$$\frac{\partial(T_0 + \text{St}T_1)}{\partial x}(0, z, t) = \frac{(T_0 + \text{St}T_1)(0, z, t)}{R(z, t)}$$

$$\frac{\partial T_0}{\partial x}(0, z, t) = \frac{T_0(0, z, t)}{R(z, t)}, \quad (3.4a)$$

$$\frac{\partial T_1}{\partial x}(0, z, t) = \frac{T_1(0, z, t)}{R(z, t)}, \quad (3.4b)$$

$$\frac{\partial(T_0 + \text{St}T_1)}{\partial x}(s_0(z, t) + \text{St}s_1(z, t), z, t) = \frac{\partial(s_0 + \text{St}s_1)}{\partial t} + \frac{\partial(s_0 + \text{St}s_1)}{\partial z}$$

$$\frac{\partial T_0}{\partial x}(s_0(z, t), z, t) = \frac{\partial s_0}{\partial t} + \frac{\partial s_0}{\partial z}, \quad (3.5a)$$

$$\frac{\partial T_1}{\partial x}(s_0(z, t), z, t) + s_1(z, t) \frac{\partial^2 T_0}{\partial x^2}(s_0(z, t), z, t) = \frac{\partial s_1}{\partial t} + \frac{\partial s_1}{\partial z}$$

$$\frac{\partial T_1}{\partial x}(s_0(z, t), z, t) = \frac{\partial s_1}{\partial t} + \frac{\partial s_1}{\partial z}, \quad (3.5b)$$

$$(T_0 + \text{St}T_1)(s_0(z, t) + \text{St}s_1(z, t), z, t) = 1$$

$$T_0(s_0(z, t), z, t) = 1, \quad (3.6a)$$

$$s_1(z, t) \frac{\partial T_0}{\partial x}(s_0(z, t), z, t) + T_1(s_0(z, t), z, t) = 0, \quad (3.6b)$$

where we have used (3.3a) when deriving (3.5b).

Solving (3.3a) subject to (3.4a) and (3.6a), we have the following:

$$\begin{aligned} T_0(x, z, t) &= A_1(z, t)x + A_2(z, t) \\ &= A_1(z, t)(x - s) + 1 \\ &= \frac{x + R(z, t)}{s_0 + R(z, t)}. \end{aligned} \quad (3.7)$$

Substituting the above into (3.5a), we obtain

$$\frac{\partial s_0}{\partial t} + \frac{\partial s_0}{\partial z} = \frac{1}{s_0 + R(z, t)}. \quad (3.8)$$

The function R depends on deviations in the contact pressure from hydrostatic pressure. If these deviations are small (in some appropriate scaling, presented in §6), then R may be approximated by a constant. (Note that with our definition of h , the constant should be $R = 1$. However, we leave R arbitrary for now.) Then (3.8) becomes

$$\begin{aligned} (s_0 + R) \left(\frac{\partial s_0}{\partial t} + \frac{\partial s_0}{\partial z} \right) &= 1 \\ (s_0 + R) \frac{ds_0}{dz} &= 1 \quad \text{when} \quad \frac{dt}{dz} = 1 \\ \frac{s_0^2}{2} + Rs_0 &= z + A, \\ s_0(z, t) &= -R + \sqrt{R^2 + 2(z + A)}. \end{aligned}$$

To solve for A , we note that the front always initiates at the liquid-air interface, so we have

$$s_0(0, t) = 0 \quad \implies \quad A = 0,$$

and hence we obtain

$$s_0(z, t) = -R + \sqrt{R^2 + 2z}. \quad (3.9)$$

This solution actually covers two cases. In the steady case, there is no dependence on t at all and (3.9) holds for $z \geq 0$. In the unsteady case, we impinge the flow into the melt at $t = 0$. Therefore, the domain is $0 \leq z \leq t$, but (3.9) still holds. This corresponds to a wedge developing with the wide end at the entering end of the mold (see Fig. 1). Here we

have neglected edge effects which would smooth the sharp edge. Substituting (3.9) into (3.7) in the case of constant R yields

$$T_0(x, z, t) = \frac{x + R}{\sqrt{R^2 + 2z}}. \quad (3.10)$$

For comparison with later work, we expand (3.9) for small z :

$$s_0(z) = -R + R\sqrt{1 + \frac{2z}{R^2}} \sim -R + R \left[1 + \frac{1}{2} \left(\frac{2z}{R^2} \right) - \frac{1}{8} \left(\frac{2z}{R^2} \right)^2 \right] = \frac{z}{R} - \frac{z^2}{2R^3}. \quad (3.11)$$

From (3.11) we note that for small z we have that the relevant x values are also $O(z)$. Keeping this in mind, we expand (3.10) to obtain a small z -and- x expansion:

$$T_0(x, z, t) = \frac{x + R}{R\sqrt{1 + 2z/R^2}} \sim \left(1 + \frac{x}{R} \right) \left(1 - \frac{z}{R^2} \right) \sim 1 + \frac{x}{R} - \frac{z}{R^2}. \quad (3.12)$$

To obtain the $O(\text{St})$ correction in the steady case, we substitute (3.7) and (3.8) into (3.3b) and (3.6b), which yields

$$\frac{\partial^2 T_1}{\partial x^2} = -\frac{x + R}{(s_0 + R)^3}, \quad (3.13a)$$

$$T_1(s_0(z), z) = -\frac{s_1}{s_0 + R}, \quad (3.13b)$$

Solving (3.13a) subject to (3.13b) and (3.4b), we obtain

$$\begin{aligned} T_1(x, z) &= -\frac{(x + R)^3}{6(s_0 + R)^3} + \frac{1}{6} - \frac{s_1}{s_0 + R} + A(x - s_0) \\ &= \frac{x + R}{s_0 + R} \left\{ \frac{1}{6} \left[1 - \frac{(x + R)^2}{(s_0 + R)^2} \right] - \frac{s_1}{s_0 + R} \right\} + \frac{R^3(x - s_0)}{3(s_0 + R)^4}. \end{aligned} \quad (3.14)$$

Substituting (3.14) into (3.5b), we have the following:

$$\begin{aligned} \frac{ds_1}{dz} &= \frac{1}{3(s_0 + R)} \left[\frac{R^3}{(s_0 + R)^3} - 1 \right] - \frac{s_1}{(s_0 + R)^2} \\ (s_0 + R) \frac{ds_1}{dz} + \frac{s_1}{s_0 + R} &= \frac{1}{3} \left[\frac{R^3}{(s_0 + R)^3} - 1 \right]. \end{aligned} \quad (3.15)$$

To integrate (3.15), we note the following identity, which follows from the steady form of (3.8):

$$\frac{d^2 s_0}{dz^2} = -\frac{1}{(s_0 + R)^2} \frac{ds_0}{dz} = -\frac{1}{(s_0 + R)^3}. \quad (3.16)$$

Substituting various permutations of (3.8) and (3.16) into (3.15), we obtain

$$\frac{ds_1}{dz} \left(\frac{ds_0}{dz} \right)^{-1} - s_1 \frac{d^2 s_0}{dz^2} \left(\frac{ds_0}{dz} \right)^{-2} = -\frac{1}{3} \left(R^3 \frac{d^2 s_0}{dz^2} + 1 \right) \quad (3.17a)$$

$$s_1 \left(\frac{ds_0}{dz} \right)^{-1} = -\frac{1}{3} \left(R^3 \frac{ds_0}{dz} + z + A \right)$$

$$s_1(z) = -\frac{1}{3(s_0 + R)} \left(\frac{R^3}{s_0 + R} + z - R^2 \right), \quad (3.17b)$$

where we have used the fact that $s_1(0) = 0$. Substituting in the form of $s_0(z)$ from (3.9), we have the following:

$$s_1(z) = -\frac{1}{3\sqrt{R^2 + 2z}} \left(\frac{R^3}{\sqrt{R^2 + 2z}} + z - R^2 \right). \quad (3.18)$$

Substituting (3.9) and (3.18) into (3.14), we obtain

$$T_1(x, z) = \frac{x + R}{\sqrt{R^2 + 2z}} \left\{ \frac{1}{6} \left[1 - \frac{(x + R)^2}{R^2 + 2z} \right] - \frac{s_1}{s_0 + R} \right\} + \frac{R^3(x - \sqrt{R^2 + 2z})}{3(R^2 + 2z)^2} \quad (3.19a)$$

$$= \frac{x + R}{\sqrt{R^2 + 2z}} \left\{ \frac{1}{6} \left[1 - \frac{(x + R)^2}{R^2 + 2z} \right] + \frac{1}{3(R^2 + 2z)} \left(\frac{R^3}{\sqrt{R^2 + 2z}} + z - R^2 \right) \right\}$$

$$+ \frac{R^3(x - \sqrt{R^2 + 2z})}{3(R^2 + 2z)^2}$$

$$= \frac{x + R}{\sqrt{R^2 + 2z}} \left\{ \frac{1}{6} \left[1 - \frac{(x + R)^2}{R^2 + 2z} \right] + \frac{z - R^2}{3(R^2 + 2z)} \right\} + \frac{R^3(2x + R - \sqrt{R^2 + 2z})}{3(R^2 + 2z)^2}.$$

(3.19b)

Expanding (3.18) for small z yields

$$\begin{aligned} s_1(z) &= -\frac{1}{3R\sqrt{1 + 2z/R^2}} \left(\frac{R^2}{\sqrt{1 + 2z/R^2}} + z - R^2 \right) \\ &\sim -\frac{1}{3R} \left\{ R^2 \left[1 - \frac{1}{2} \left(\frac{2z}{R^2} \right) + \frac{3}{8} \left(\frac{2z}{R^2} \right)^2 \right] + z - R^2 \right\} \\ &\sim -\frac{R}{3} \left(\frac{3z^2}{2R^4} \right) \\ &\sim -\frac{z^2}{2R^3}. \end{aligned} \quad (3.20)$$

We also expand (3.21) for small z and x , retaining only those terms which are $O(x^2) = O(z^2)$:

$$T_1(x, z) \sim -\frac{x^2}{2R^2} + \frac{z^2}{R^4} = \frac{1}{R^2} \left(\frac{z^2}{R^2} - \frac{x^2}{2} \right). \quad (3.21)$$

Therefore, for small z we have that

$$s(z) \sim \frac{z}{R} - \frac{z^2(1 + \text{St})}{2R^3}, \quad (3.22a)$$

$$T(x, z) = 1 + \frac{x}{R} - \frac{z}{R^2} + \frac{\text{St}}{R^2} \left(\frac{z^2}{R^2} - \frac{x^2}{2} \right) + O(z^2, x^2, xz). \quad (3.22b)$$

Here we have not listed all the terms in the $O(z^2)$ perturbation expansion because only the parabolic terms multiplying St will be of interest.

For the unsteady case, we note again that (3.17a) will hold on lines where $dt/dz = 1$, and hence we obtain all the same solutions, except restricted to $z \leq t$.

Section 4: Flat Surface, Moderate St

For the moderate Stefan number case, the convective boundary condition makes an exact solution difficult. However, there are several approximate methods available. We assume that $\epsilon = o(1)$ and also focus on the steady case. Therefore, equations (2.12), (2.10), (2.11), and (3.1) become, to leading order,

$$\text{St} \frac{\partial T}{\partial z} = \frac{\partial^2 T}{\partial x^2}, \quad (4.1)$$

$$\frac{\partial T}{\partial x}(s(z), z) = \frac{ds}{dz}, \quad (4.2)$$

$$T(s(z), z) = 1, \quad (4.3)$$

$$\frac{\partial T}{\partial x}(0, z) = \frac{T(0, z)}{R(z)}. \quad (4.4)$$

We begin with the Megerlin method [2]. In this method, we assume that the temperature profile is parabolic in x . Satisfying equations (4.2) and (4.3) immediately, we have

$$T_M(x, z) = 1 + \frac{ds_M}{dz}(x - s_M) + \frac{A(z)(x - s_M)^2}{2}, \quad (4.5)$$

where the subscript ‘‘M’’ (for Megerlin) emphasizes that we are going to calculate only approximations to T and s . To calculate $A(z)$, we satisfy equation (4.4):

$$\begin{aligned} \frac{ds_M}{dz} - A(z)s_M &= \frac{1}{R(z)} \left[1 - \frac{ds_M}{dz}s_M + \frac{A(z)s_M^2}{2} \right] \\ A(z) \left[R(z)s_M + \frac{s_M^2}{2} \right] &= R(z) \frac{ds_M}{dz} - 1 + s_M \frac{ds_M}{dz} \\ A(z) &= \frac{(s_M + R)ds_M/dz - 1}{s_M[R(z) + s_M/2]} \\ A(z) &= \frac{d\{s_M[R(z) + s_M/2]\}/dz - 1}{s_M[R(z) + s_M/2]}. \end{aligned} \quad (4.6)$$

In the Megerlin method, we assume that T_M satisfies (4.1) *only at* $x = s_M(z)$. Therefore, we have

$$\begin{aligned} \text{St} \frac{\partial T_M}{\partial z}(s_M(z), z) &= \frac{\partial^2 T_M}{\partial x^2}(s_M(z), z) \\ -\text{St} \left(\frac{ds_M}{dz} \right)^2 &= A(z) \\ -\text{St} \left(\frac{ds_M}{dz} \right)^2 &= \frac{[s_M + R(z)]ds_M/dz - 1}{s_M[R(z) + s_M/2]} \end{aligned} \quad (4.7a)$$

$$0 = \text{St} s_M \left[R(z) + \frac{s_M}{2} \right] \left(\frac{ds_M}{dz} \right)^2 + [s_M + R(z)] \frac{ds_M}{dz} - 1$$

$$\frac{ds_M}{dz} = \frac{-[s_M + R(z)] + \sqrt{[s_M + R(z)]^2 + 2\text{St} s_M [s_M + 2R(z)]}}{\text{St} s_M [s_M + 2R(z)]}. \quad (4.7b)$$

We believe that equations (4.7) must be solved numerically. However, we would like to obtain a small- z asymptote to see what happens near the area where the mold enters the melt. In particular, in the case of constant R we would like the small- z asymptote to match with (3.22a). Therefore, we make the following *ansatz* and see if it satisfies the leading orders of (4.7a):

$$s_M \sim \frac{z}{R} - \frac{z^2(1 + \text{St})}{2R^3}. \quad (4.8)$$

Substituting (4.8) into (4.7a) and expanding to leading order, we have

$$-\text{St} \left(\frac{1}{R} \right)^2 = \left[\left(\frac{z}{R} + R \right) \left(\frac{1}{R} - \frac{z(1 + \text{St})}{R^3} \right) - 1 \right] \left(R \frac{z}{R} \right)^{-1}$$

$$-\frac{\text{St}}{R^2} = \frac{1}{R^2} - \frac{(1 + \text{St})}{R^2}, \quad (4.9)$$

and hence we see that (4.8) is indeed correct to leading two orders. (Note that the only place where the z^2 term came into play was in the ds_M/dz term.) Since both sides of (4.9) are an asymptotic expansion for $A(z)$ for small z , we see that for small z we have

$$T_M(x, z) \sim 1 + \left(\frac{1}{R} \right) \left(x - \frac{z}{R} \right) - \frac{\text{St}}{2R^2} \left(\frac{x - z}{R} \right)^2$$

$$= 1 + \frac{x}{R} - \frac{z}{R} - \frac{\text{St}}{R^2} \left(\frac{x^2}{2} - \frac{xz}{R} + \frac{z^2}{R^2} \right), \quad (4.10)$$

which does not match with (3.22b) at $O(\text{St})$. However, several of the terms are the same, which should occur since T_M is an approximation.

Next we try the integral balance method [2]. Again we assume a parabolic profile, and since $A(z)$ was determined by satisfying the boundary conditions, (4.6) still holds with a new subscript ‘‘I’’ (for integral balance method) replacing the subscript ‘‘M’’. We require that $T_I(x, z)$ satisfy (4.1) in an average sense, so we have

$$\int_0^{s_I} \text{St} \frac{\partial T_I}{\partial z} dx = \int_0^{s_I} \frac{\partial^2 T_I}{\partial x^2} dx$$

$$\text{St} \left[\frac{\partial}{\partial z} \int_0^{s_I} T_I dx - \frac{ds_I}{dz} T_I(s_I(z), z) \right] = \int_0^{s_I} A(z) dx$$

$$\text{St} \left[\frac{d}{dz} \left(s_I - \frac{s_I^2}{2} \frac{ds_I}{dz} + A(z) \frac{s_I^3}{6} \right) - \frac{ds_I}{dz} \right] = A(z) s_I$$

$$\frac{\text{St}}{6} \left\{ \frac{d[A(z) s_I^3]}{dz} - \frac{d^2(s_I^3)}{dz^2} \right\} = A(z) s_I. \quad (4.11)$$

In general, (4.11) must be solved numerically. Since it is a second-order equation for s_I , we need a derivative condition as well as the condition that $s_I(0) = 0$.

This condition can be derived from a small- z expansion. Again, for the case of constant R we try to match (3.22a) by assuming that

$$s_I \sim \frac{z}{R} - \frac{z^2(1 + \text{St})}{2R^3}. \quad (4.12)$$

Substituting (4.12) into (4.11) and retaining terms to leading order, we have

$$\begin{aligned} \frac{\text{St}}{6} \left[\frac{\partial}{\partial z} \left(-\frac{\text{St}}{R^2} \frac{z^3}{R^3} \right) - \frac{\partial^2}{\partial z^2} \left(\frac{z^3}{R^3} \right) \right] &= -\frac{\text{St}}{R^2} \frac{z}{R} \\ -\frac{\text{St}z}{R^3} &= -\frac{\text{St}z}{R^3}, \end{aligned}$$

where we have used the second term in the expansion when we replace $A(z)$ by $-\text{St}/R^2$. Therefore, we see that (4.12) holds for s_I and the second condition for (4.11) is

$$\frac{ds_I}{dz}(0) = \frac{1}{R}. \quad (4.13)$$

Also, since the small- z asymptote for s_I is the same as for s_M , we see that our small- z asymptote for T_M in (4.10) also holds for T_I .

We note that throughout this section we have considered the steady case. Looking at the unsteady case may be more complicated due to the nature of the partial differential equation we are attempting to solve.

Section 5: The Influence of Mold Topography

We now examine the influence of mold topography on location of the solidification front, assuming a topography with a single frequency; see Fig. 3. Therefore, we have the following form for \tilde{x}_s :

$$\tilde{x}_s = \tilde{a} \cos\left(\frac{\tilde{z} - V\tilde{t}}{\tilde{\ell}}\right). \quad (5.1)$$

Normalizing as before, we have

$$x_s = a \cos\left(\frac{z - t}{\epsilon\ell}\right) \quad (5.2)$$

where

$$a = \frac{\tilde{a}}{x_c}, \quad \ell = \frac{\tilde{\ell}}{x_c},$$

Using the parameters in the Appendix, we find that $a = 4.1 \times 10^{-5} \ll 1$.

The experiments on effects of mold topography include surface irregularities over a wide range of frequencies. We consider two cases: that of long-range ‘undulations’ and that of small-scale ‘surface roughness.’

Undulations

We first consider the case of long-range ‘undulations’ where

$$\tilde{\ell} = 2 \text{ cm} \quad \implies \quad \ell = 0.83.$$

Substituting (5.2) into (2.7b), we obtain the mold surface boundary condition

$$\left[1 + \frac{a^2}{\ell^2} \sin^2\left(\frac{z - t}{\epsilon\ell}\right)\right]^{-1/2} \left[\frac{\partial T}{\partial x} + \frac{\epsilon a}{\ell} \sin\left(\frac{z - t}{\epsilon\ell}\right) \frac{\partial T}{\partial z}\right] = \frac{T}{R} \text{ at } x = x_s. \quad (5.3)$$

We note that equations (2.10), (2.11) and (2.12) remain unchanged. Our task is thus to solve (2.10)–(2.12) with the new mold surface boundary condition (5.3). The system differs from that considered earlier in §§3 and 4 in that (5.3) introduces a new length scale in the z -direction, defined by the length scale of undulations on the mold surface. This length scale manifests itself through the appearance of a new, fast variable $\eta = (z - t)/\epsilon$, where $\epsilon \ll 1$.

To develop an asymptotic approximation to the solution of this problem, we use a multiple-scale method with the Stefan number as our small parameter. In order to write all our parameters in terms of the Stefan number, we assume that

$$\epsilon = O(\text{St}), \quad a = a_0 \text{St} + O(\text{St}^2).$$

We need not write an explicit series for ϵ since with the inclusion of η , ϵ will drop out of our problem to leading two orders. The latter assumption reaffirms that the amplitude of the undulations on the mold surface is small. Next, we seek a solution in the form of a series in St , and we explicitly include the fast variable η by putting

$$T(x, z, t) \sim T_0(x, z, t) + \text{St}T_1(x, z, t, \eta) + O(\text{St}^2), \quad s(z, t) \sim s_0(z, t) + \text{St}s_1(z, t, \eta) + O(\text{St}^2).$$

We treat η as an independent variable, substituting our expansions for T and s into the governing equations (2.10)–(2.12) and (5.3). Then we equate coefficients of like powers of St to obtain a sequence of systems which determine T_n and s_n sequentially. The dependence of T and s on η is absent at leading order, and appears only at the next order ($O(\text{St})$). This is a simple consequence of the assumption that the amplitude a of the surface topography is small. To leading order, the mold surface appears flat, and we expect our results to agree with those of §3. On the other hand, at $O(\text{St})$ the fast variable η enters the problem through the boundary condition (5.3), so that η -dependence must be included at this order. The systems at the first two orders are therefore sufficient to capture the dominant effect of mold topography.

At leading order ($O(1)$), we have

$$\frac{\partial^2 T_0}{\partial x^2} = 0, \tag{5.4}$$

$$\frac{\partial T_0}{\partial x}(0, z, t) = \frac{T_0}{R}(0, z, t), \tag{5.5}$$

$$T_0(s_0, z, t) = 1, \tag{5.6a}$$

$$\frac{\partial T_0}{\partial x}(s_0, z, t) = \frac{\partial s_0}{\partial t} + \frac{\partial s_0}{\partial z}, \tag{5.6b}$$

while at $O(\text{St})$ we have

$$\frac{\partial^2 T_1}{\partial x^2} + \frac{\partial^2 T_1}{\partial \eta^2} = \frac{\partial T_0}{\partial t} + \frac{\partial T_0}{\partial z}, \tag{5.7}$$

$$\frac{\partial T_1}{\partial x}(0, z, t, \eta) + a_0 \cos(\eta/\ell) \frac{\partial^2 T_0}{\partial x^2}(0, z, t) = \frac{T_1(0, z, t, \eta)}{R} + a_0 \cos(\eta/\ell) \frac{\partial T_0}{\partial x}(0, z, t), \tag{5.8}$$

$$\frac{\partial T_1}{\partial x}(s_0, z, t, \eta) + s_1 \frac{\partial^2 T_0}{\partial x^2}(s_0, z, t) = \frac{\partial s_1}{\partial t} + \frac{\partial s_1}{\partial z}, \tag{5.9a}$$

$$T_1(s_0, z, t, \eta) + s_1 \frac{\partial T_0}{\partial x}(s_0, z, t) = 0. \tag{5.9b}$$

The solution of the leading-order system (5.4)–(5.6b) is given by equations (3.7) and (3.9). Hence, we turn to the system (5.7)–(5.9b) and use the leading-order solution to simplify it. We obtain

$$\frac{\partial^2 T_1}{\partial x^2} + \frac{\partial^2 T_1}{\partial \eta^2} = \frac{\partial T_0}{\partial z}, \tag{5.10}$$

$$\frac{\partial T_1}{\partial x}(0, z, t, \eta) - \frac{T_1(0, z, t, \eta)}{R} = \frac{a_0}{R} \cos(\eta/l) \frac{1}{s_0 + R}, \quad (5.11)$$

$$T_1(s_0, z, t, \eta) + \frac{s_1}{s_0 + R} = 0, \quad (5.12a)$$

$$\frac{\partial T_1}{\partial x}(s_0, z, t, \eta) = \frac{\partial s_1}{\partial t} + \frac{\partial s_1}{\partial z}. \quad (5.12b)$$

Since the system (5.10)–(5.12b) is linear in T_1 and s_1 , we may decompose its solution into a sum. Hence, we seek solutions of the form

$$T_1(x, z, t, \eta) = T_m(x, z, t) \cos(\eta/l) + T_{\text{flat}}(x, z, t), \quad (5.13a)$$

$$s_1(z, t, \eta) = s_m(z, t) \cos(\eta/l) + s_{\text{flat}}(z, t), \quad (5.13b)$$

where the subscript “m” refers to the contribution due to mold topography and the subscript “flat” refers to the contribution due to the influence of non-zero Stefan number on the flat mold solution. Thus we choose T_{flat} and s_{flat} so that they satisfy the perturbed flat mold problem. That is, T_{flat} and s_{flat} are chosen to satisfy the flat mold problem at order $O(\text{St})$ as found in §3. Simplifying that system ((3.3b), (3.4b), (3.5b), and (3.6b)) somewhat, we see that T_{flat} and s_{flat} satisfy

$$\frac{\partial^2 T_{\text{flat}}}{\partial x^2} = \frac{\partial T_0}{\partial z}, \quad (5.14)$$

$$\frac{\partial T_{\text{flat}}}{\partial x}(0, z, t) = \frac{T_{\text{flat}}(0, z, t)}{R}, \quad (5.15)$$

$$T_{\text{flat}}(s_0, z, t) + \frac{s_{\text{flat}}(z, t)}{s_0 + R} = 0, \quad (5.16a)$$

$$\frac{\partial T_{\text{flat}}}{\partial x}(s_0, z, t) = \frac{\partial s_{\text{flat}}}{\partial t} + \frac{\partial s_{\text{flat}}}{\partial z}. \quad (5.16b)$$

Similarly, T_m and s_m satisfy

$$\frac{\partial^2 T_m}{\partial x^2} - \frac{T_m}{\ell} = 0, \quad (5.17)$$

$$\frac{\partial T_m}{\partial x}(0, z, t) = \frac{T_m(0, z, t)}{R} + \frac{a_0}{R(s_0 + R)}, \quad (5.18)$$

$$\frac{\partial T_m}{\partial x}(s_0, z, t) = \frac{\partial s_m}{\partial t} + \frac{\partial s_m}{\partial z}, \quad (5.19a)$$

$$T_m(s_0, z, t) + \frac{s_m}{s_0 + R} = 0. \quad (5.19b)$$

We solve the system (5.17)–(5.19b) for T_m and eliminate terms to obtain an equation in s_m only. In this manner, we find the following partial differential equation for s_m , which

governs the amplitude of the η -dependent perturbation to the moving boundary at order $O(\text{St})$:

$$\begin{aligned} \frac{\partial s_m}{\partial t} + \frac{\partial s_m}{\partial z} + \frac{\cosh(s_0/\ell) + (R/\ell) \sinh(s_0/\ell)}{R(s_0 + R)(\cosh(s_0/\ell) + (\ell/R) \sinh(s_0/\ell))} s_m \\ = \frac{a_0}{R(s_0 + R)(\cosh(s_0/\ell) + (\ell/R) \sinh(s_0/\ell))}. \end{aligned} \quad (5.20)$$

Since we are interested in macroscopic irregularities in the cast surface, we examine the behavior of the solution of (5.20) for s_m when z and t are large. Along characteristics $dz/dt = 1$ of (5.20), $s_0 \sim \sqrt{2t}$, so we find that s_m satisfies

$$\frac{ds_m}{dt} + \frac{Rs_m}{\ell^2 \sqrt{2t}} = 0,$$

Thus, s_m decays exponentially along characteristics as z and t tend to ∞ . The physical implications are clear: initially, *i.e.*, near the point where the mold surface enters the solidifying melt, the solidification front exhibits small-amplitude undulations that conform to the mold surface topography, but their amplitude decreases at points on the front that are further into the melt, where the time over which solidification has occurred is greater.

Tip Dynamics

We next examine the case of surface roughness where, using the values in the Appendix,

$$\ell = 2.08 \times 10^{-2}.$$

Clearly the introduction of the undulations introduces a new length scale $\epsilon\ell$ for \tilde{z} (and hence a new scale for \tilde{t}). Since a is so small, we note from the above analysis that far from the tip where $s(0, t) = 0$, the undulations do not contribute appreciably to the dynamics. However, near the tip they may contribute.

To examine the tip dynamics, we introduce the following new variables:

$$T(x, z, t) = \theta_0(\xi, \zeta, \tau) + \epsilon\ell\theta_1(\xi, \zeta, \tau) + o(1), \quad s(z, t) = x_\ell S(\zeta, \tau) + o(1), \quad (5.21a)$$

$$\xi = \frac{x}{x_\ell}, \quad \zeta = \frac{z}{\epsilon\ell}, \quad \tau = \frac{t}{\epsilon\ell}, \quad (5.21b)$$

where x_ℓ is yet to be determined. However, we note from (3.11) that in the steady case near the tip we have

$$s(z) \sim \frac{z}{R} = \frac{\epsilon\ell\zeta}{R}.$$

Thus, we set $x_\ell = \epsilon\ell$.

Making these substitutions into (2.12), (2.10), (2.11), and (5.3), we obtain, to leading order,

$$\frac{\text{St}}{\epsilon\ell} \left(\frac{\partial(\theta_0 + \epsilon\ell\theta_1)}{\partial\tau} + \frac{\partial(\theta_0 + \epsilon\ell\theta_1)}{\partial\zeta} \right) = \frac{1}{\epsilon^2\ell^2} \left(\frac{\partial^2(\theta_0 + \epsilon\ell\theta_1)}{\partial\xi^2} + \epsilon^2 \frac{\partial^2(\theta_0 + \epsilon\ell\theta_1)}{\partial\zeta^2} \right), \quad (5.22a)$$

$$\frac{\partial^2\theta_0}{\partial\xi^2} = 0, \quad (5.22b)$$

$$\left[\frac{1}{\epsilon\ell} \frac{\partial(\theta_0 + \epsilon\ell\theta_1)}{\partial\xi} - \frac{1}{\epsilon\ell} \epsilon^2 \frac{\partial S}{\partial\zeta} \frac{\partial(\theta_0 + \epsilon\ell\theta_1)}{\partial\zeta} \right] (S(\zeta, \tau), \zeta, \tau) = \frac{\partial S}{\partial\zeta} + \frac{\partial S}{\partial\tau} \quad (5.23a)$$

$$\frac{\partial\theta_0}{\partial\xi} (S(\zeta, \tau), \zeta, \tau) = 0, \quad (5.23b)$$

$$(\theta_0 + \epsilon\ell\theta_1)(S(\zeta, \tau), \zeta, \tau) = 1 \quad (5.24a)$$

$$\theta_0(S(\zeta, \tau), \zeta, \tau) = 1, \quad (5.24b)$$

$$\begin{aligned} & \left[1 + \frac{a^2}{\ell^2} \sin^2(\zeta - \tau) \right]^{-1/2} \times \\ & \left(\frac{1}{\epsilon\ell} \frac{\partial(\theta_0 + \epsilon\ell\theta_1)}{\partial\xi} + \frac{a}{\ell^2} \sin(\zeta - \tau) \frac{\partial(\theta_0 + \epsilon\ell\theta_1)}{\partial\zeta} \right) \left(\frac{a}{\epsilon\ell} \cos(\zeta - \tau), \zeta, \tau \right) \\ & = \frac{1}{R} (\theta_0 + \epsilon\ell\theta_1) \left(\frac{a}{\epsilon\ell} \cos(\zeta - \tau), \zeta, \tau \right) \end{aligned} \quad (5.25a)$$

$$\frac{\partial\theta_0}{\partial\xi} \left(\frac{a}{\ell} \cos(\zeta - \tau), \zeta, \tau \right) = 0, \quad (5.25b)$$

where in (5.25b) we have used the fact that $a/\ell \ll 1$.

But the solution of (5.22b), (5.23b), (5.24b), and (5.25b) is

$$\theta_0(\xi, \zeta, \tau) \equiv 1, \quad (5.26)$$

and hence we have obtained the physically obvious fact that the temperature in the tip doesn't vary much from the freezing temperature. Substituting (5.26) into (5.22a), (5.23a), (5.24a), and (5.25a), we see that the next order equations are

$$\frac{\partial^2\theta_1}{\partial\xi^2} = 0, \quad (5.27)$$

$$\frac{\partial\theta_1}{\partial\xi} (S(\zeta, \tau), \zeta, \tau) = \frac{\partial S}{\partial\zeta} + \frac{\partial S}{\partial\tau}, \quad (5.28a)$$

$$\theta_1(S(\zeta, \tau), \zeta, \tau) = 0, \quad (5.28b)$$

$$\frac{\partial\theta_1}{\partial\xi} \left(\frac{a}{\ell} \cos(\zeta - \tau), \zeta, \tau \right) = \frac{1}{R}. \quad (5.29)$$

Those working on the tip dynamics proceeded no further than these equations.

Section 6: The Thermoelastic Problem

We now consider the problem for the thermal stresses in the solidified metal layer. The novel feature is that these are coupled to the thermal problem considered in the previous sections through the *thermal contact resistance* \tilde{R} , which is an experimentally-determined function of the pressure exerted by the metal on the mold. Heuristically speaking, the heat transfer between the two solids increases if they are pushed together, since the effective contact area (including asperities) increases. What experimental evidence exists [4] suggests a power-law dependence of the heat transfer coefficient $1/\tilde{R}$ on the pressure \tilde{p} , but for simplicity we make the simpler assumption of linear dependence.

We denote the stress tensor by $\tilde{\sigma}$; a local stress balance shows that its components must satisfy

$$\frac{\partial \tilde{\sigma}_{\tilde{x}\tilde{x}}}{\partial \tilde{x}} + \frac{\partial \tilde{\sigma}_{\tilde{x}\tilde{z}}}{\partial \tilde{z}} = 0, \quad \frac{\partial \tilde{\sigma}_{\tilde{x}\tilde{z}}}{\partial \tilde{x}} + \frac{\partial \tilde{\sigma}_{\tilde{z}\tilde{z}}}{\partial \tilde{z}} = -\rho g, \quad (6.1)$$

where g is the acceleration due to gravity. Thus we can write $\tilde{\sigma}$ in terms of an *Airy stress function* $\tilde{\phi}$, first subtracting the hydrostatic pressure:

$$\tilde{\sigma}_{\tilde{x}\tilde{x}} = -\rho g \tilde{z} + \frac{\partial^2 \tilde{\phi}}{\partial \tilde{z}^2}, \quad \tilde{\sigma}_{\tilde{x}\tilde{z}} = -\frac{\partial^2 \tilde{\phi}}{\partial \tilde{x} \partial \tilde{z}}, \quad \tilde{\sigma}_{\tilde{z}\tilde{z}} = -\rho g \tilde{z} + \frac{\partial^2 \tilde{\phi}}{\partial \tilde{x}^2}. \quad (6.2)$$

To close the problem we must specify a constitutive law relating $\tilde{\sigma}$ to the displacement field (\tilde{u}, \tilde{w}) . We use the equations of linear *hypo-thermo-elasticity*, namely

$$\frac{\partial \tilde{\sigma}_{\tilde{x}\tilde{x}}}{\partial \tilde{t}} = (\lambda + 2\mu) \frac{\partial^2 \tilde{u}}{\partial \tilde{x} \partial \tilde{t}} + \lambda \frac{\partial^2 \tilde{w}}{\partial \tilde{z} \partial \tilde{t}} - 2(\lambda + \mu) \alpha \frac{\partial \tilde{T}}{\partial \tilde{t}}, \quad (6.3a)$$

$$\frac{\partial \tilde{\sigma}_{\tilde{x}\tilde{z}}}{\partial \tilde{t}} = \mu \frac{\partial^2 \tilde{u}}{\partial \tilde{z} \partial \tilde{t}} + \mu \frac{\partial^2 \tilde{w}}{\partial \tilde{x} \partial \tilde{t}}, \quad (6.3b)$$

$$\frac{\partial \tilde{\sigma}_{\tilde{z}\tilde{z}}}{\partial \tilde{t}} = (\lambda + 2\mu) \frac{\partial^2 \tilde{w}}{\partial \tilde{z} \partial \tilde{t}} + \lambda \frac{\partial^2 \tilde{u}}{\partial \tilde{x} \partial \tilde{t}} - 2(\lambda + \mu) \alpha \frac{\partial \tilde{T}}{\partial \tilde{t}}, \quad (6.3c)$$

where λ and μ are the Lamé constants and α is the coefficient of thermal expansion. Thermal stress are purely dilational, so they appear only in (6.3a) and (6.3c).

Equations (6.3) are simply the result of differentiating the left- and right-hand sides of the usual thermo-elastic constitutive relation with respect to \tilde{t} . The rationale for this is that the equilibrium state, at which the stress is purely hydrostatic, is fixed at the freezing front and hence unknown *a priori*. The equilibrium state can be associated with the three arbitrary functions of \tilde{x} and \tilde{z} that are introduced if (6.3) is integrated with respect to \tilde{t} . With the three extra degrees of freedom (six in a three-dimensional geometry) come three more boundary conditions at the freezing front. Firstly the stress is purely hydrostatic: this supplies one more boundary condition than in classical elasticity, where only the normal component of stress is specified at a free boundary. Secondly, the material at the freezing

front is at its equilibrium state and so the displacement there is zero. (One can readily verify that the same count works in three dimensions: specifying the stress gives three extra conditions, which along with specifying the three components of displacement yields six extra conditions for the six extra degrees of freedom.)

We wish to scale our problem by the largest characteristic stress around; that way all the dimensionless stresses will be $O(1)$ or less. By looking for a leading-order balance in (6.3) we obtain the appropriate scalings for the displacement and stress, namely

$$\tilde{u}(\tilde{x}, \tilde{z}, \tilde{t}) = \alpha x_c \Delta T u(x, z, t), \quad \tilde{w}(\tilde{x}, \tilde{z}, \tilde{t}) = \alpha z_c \Delta T w(x, z, t), \quad (6.4a)$$

$$\tilde{\sigma}(\tilde{x}, \tilde{z}, \tilde{t}) = 2(\lambda + \mu)\alpha \Delta T \sigma(x, z, t), \quad (6.4b)$$

where σ , u , and w are dimensionless. Using the parameter values given in the Appendix, the typical strain $\alpha \Delta T$ is around 2.4% and the typical stress $\alpha E \Delta T \approx 1.4 \times 10^9$ Pa, where E is the Young's modulus. The latter seems rather large, and it was suggested at the meeting that in the temperature range of interest, E may be somewhat smaller than the value quoted in the Appendix (which we understand to have been measured at room temperature).

Finally, the appropriate scaling for the Airy stress function is

$$\tilde{\phi}(\tilde{x}, \tilde{z}, \tilde{t}) = 2(\lambda + \mu)x_c^2 \alpha \Delta T \phi(x, z, t). \quad (6.4c)$$

In writing the equations (6.3) in dimensionless form we look for a steady solution in our moving frame, so that derivatives with respect to \tilde{t} are replaced by those with respect to \tilde{z} via $\partial/\partial \tilde{t} = V \partial/\partial \tilde{z}$. Since the \tilde{t} -derivative appears in each term, the V s cancel and hence we arrive at the following three equations for ϕ , u and w :

$$-\epsilon^2 B + \epsilon^2 \frac{\partial^3 \phi}{\partial z^3} = (1 - \nu) \frac{\partial^2 u}{\partial x \partial z} + \nu \frac{\partial^2 w}{\partial z^2} - \frac{\partial T}{\partial z}, \quad (6.5a)$$

$$-\epsilon^2 \frac{\partial^3 \phi}{\partial x \partial z^2} = \left(\frac{1}{2} - \nu\right) \left(\frac{\partial^2 w}{\partial x \partial z} + \epsilon^2 \frac{\partial^2 u}{\partial z^2} \right), \quad (6.5b)$$

$$-\epsilon^2 B + \frac{\partial^3 \phi}{\partial x^2 \partial z} = (1 - \nu) \frac{\partial^2 w}{\partial z^2} + \nu \frac{\partial^2 u}{\partial x \partial z} - \frac{\partial T}{\partial z}, \quad (6.5c)$$

where ν is Poisson's ratio and B is a dimensionless parameter measuring the relative influence of hydrostatic pressure and thermal stress:

$$B = \frac{\rho g z_c^3}{2x_c^2(\lambda + \mu)\alpha \Delta T} = \frac{\rho g z_c^3(1 + \nu)(1 - 2\nu)}{x_c^2 \alpha E \Delta T}. \quad (6.6)$$

The parameter values in the Appendix suggest that B is small: around 2×10^{-3} , which would imply that hydrostatic pressure is negligible compared to thermal stresses. However, as mentioned above, there is some uncertainty as to the true value of E . Notice moreover that the length-scales z_c and x_c are defined in terms of the heat-transfer coefficient h . Since in this section the heat transfer is *not* assumed to be constant (it depends on the

contact pressure) it is not immediately clear how to define h uniquely: we address this issue in more detail later. So for the moment we proceed treating B as an $O(1)$ constant.

Now we must consider suitable boundary conditions to apply to (6.5). As outlined above, on the free boundary $x = s(z)$ we have zero displacement:

$$u = w = 0 \quad \text{on } x = s(z), \quad (6.7)$$

and the stress tensor is purely hydrostatic. From the dimensionless form of (6.2) we see that this implies that

$$\frac{\partial^2 \phi}{\partial x \partial z} = 0 \quad \text{on } x = s(z), \quad (6.8a)$$

$$\frac{\partial^2 \phi}{\partial z^2} = 0 \quad \text{on } x = s(z). \quad (6.8b)$$

Since on the curve $x = s(z)$ all the functions in (6.8) depend on z only, we may integrate (6.8b) once with respect to z to see that $\partial\phi/\partial z$ is a constant A at the freezing surface. However, we see from the dimensionless form of (6.2) that we may add an arbitrary linear function of z to our solution ϕ without changing the resulting stress field σ . Hence we may set $A = 0$, thereby replacing (6.8b) with

$$\frac{\partial \phi}{\partial z} = 0 \quad \text{on } x = s(z). \quad (6.9)$$

This sort of integration trick may also be used on (6.10) and (6.9a) to yield the more standard conditions

$$\phi = \frac{\partial \phi}{\partial x} = \frac{\partial^2 \phi}{\partial x^2} = 0 \quad \text{on } x = s(z),$$

where we have used the form for σ_{zz} at the interface. However, these boundary conditions are not in a useful form for our problem.

The correct boundary conditions to be imposed on the mold (which we choose to be flat, so $x_s = 0$) are less clear, since the form of mechanical contact between the metal and the mold is uncertain. We consider two possible scenarios. Firstly, if we assume that the metal remains in contact with the mold everywhere, and that the tangential stress there is zero, then we impose

$$\textbf{zero friction:} \quad u = \frac{\partial^2 \phi}{\partial x \partial z} = 0 \quad \text{on } x = 0. \quad (6.10a)$$

This condition is probably not particularly realistic. There must be some kind of traction between the mold and the metal since we know that the metal is dragged along by the mold. However, (6.10a) makes the solution of the problem particularly simple, and might be expected to give qualitatively correct results. Also, this boundary condition was previously imposed in a similar context in [5].

Secondly, an arguably more physically relevant condition is to impose zero slip between the metal and the mold:

$$\textbf{zero slip:} \quad u = w = 0 \quad \text{on } x = 0. \quad (6.10b)$$

It might be more realistic still, though considerably more complicated, to impose a Coulomb friction law. Also, we really ought to pose an elastic contact problem in which $u = 0$ when the contact pressure is positive and $u > 0$ when the pressure is zero (*i.e.* when the metal loses contact with the mold).

The equations (6.5) with their associated boundary conditions (6.7), (6.8a), (6.9), and either of (6.10) in principle enable us to find the displacements and stresses in the solid layer *if the temperature distribution T and free boundary s are known*. For simplicity we concentrate here on the zero Stefan number limit, in which T and s are given to leading order by

$$T_0 = \frac{x + R}{s_0 + R}, \quad \frac{ds_0}{dz} = \frac{1}{s_0 + R}. \quad (6.11)$$

Recall that the coupling between the thermal and elastic problems is in the contact resistance R , which depends on the pressure exerted by the metal on the mold. Thus the problem is closed by specifying a constitutive law $R = R(p)$, where p is the dimensionless pressure exerted by the metal on the mold. The dimensional pressure is the negative of the normal stress $\tilde{\sigma}_{\tilde{x}\tilde{x}}$ on the surface of the mold, and hence we have

$$\begin{aligned} \tilde{p}(\tilde{z}) &= \rho g \tilde{z} - \frac{\partial^2 \tilde{\phi}}{\partial \tilde{z}^2}(0, \tilde{z}) \\ p(z) &= Bz - \frac{\partial^2 \phi}{\partial z^2}(0, z), \\ \tilde{p}(\tilde{z}) &= 2\epsilon^2(\lambda + \mu)\alpha\Delta T p(z). \end{aligned} \quad (6.12)$$

The values given in the Appendix suggest that the typical pressure scale is around 10^7 Pa.

The equations (6.5) with their associated boundary conditions (6.7), (6.8a), (6.9), and either of (6.10) appear rather formidable, but they have the following fortunate property. To close the problem for T and the free boundary s we need to find only the pressure p , and *we can do so without solving for the displacements u and w* . The solution is clarified by introducing the substitutions

$$\frac{\partial \phi}{\partial z} = \Phi(x, z; \epsilon, \text{St}) = \Phi_0(x, z) + o(1), \quad \frac{\partial u}{\partial z} = U(x, z; \epsilon, \text{St}) = U_0(x, z) + o(1), \quad (6.13a)$$

$$\frac{\partial w}{\partial z} = W(x, z; \epsilon, \text{St}) = W_0(x, z) + o(1). \quad (6.13b)$$

Note that we do not indicate the next term in the expansion [it will probably be $O(\text{St})$, since we are also taking $\text{St} \rightarrow 0$]. Substituting (6.13) into (6.5), (6.8a), (6.19), and (6.10), we obtain the leading-order problem

$$0 = (1 - \nu) \frac{\partial U_0}{\partial x} + \nu \frac{\partial W_0}{\partial z} - \frac{\partial T_0}{\partial z}, \quad (6.14a)$$

$$0 = \left(\frac{1}{2} - \nu\right) \frac{\partial W_0}{\partial x}, \quad (6.14b)$$

$$\frac{\partial^2 \Phi_0}{\partial x^2} = (1 - \nu) \frac{\partial W_0}{\partial z} + \nu \frac{\partial U_0}{\partial x} - \frac{\partial T_0}{\partial z}, \quad (6.14c)$$

$$\Phi_0 = \frac{\partial \Phi_0}{\partial x} = 0 \quad \text{on } x = s_0(z), \quad (6.15)$$

$$U_0 = \frac{\partial \Phi_0}{\partial x} = 0 \quad \text{on } x = 0, \quad (6.16a)$$

$$U_0 = W_0 = 0 \quad \text{on } x = 0. \quad (6.16b)$$

First we observe from (6.14b) that W_0 is independent of x :

$$W_0 = W_0(z). \quad (6.17)$$

Then from (6.14a) we read off $\partial U_0 / \partial x$,

$$\frac{\partial U_0}{\partial x} = \frac{1}{1-\nu} \frac{\partial T_0}{\partial z} - \frac{\nu}{1-\nu} \frac{dW_0}{dz},$$

and substitute it into (6.14c):

$$\frac{\partial^2 \Phi_0}{\partial x^2} = \left(\frac{1-2\nu}{1-\nu} \right) \left(\frac{dW_0}{dz} - \frac{\partial T_0}{\partial z} \right). \quad (6.18)$$

Integrating (6.18) once using the derivative condition in (6.15), we obtain

$$\frac{\partial \Phi_0}{\partial x} = \left(\frac{1-2\nu}{1-\nu} \right) \left[(x-s_0) \frac{dW_0}{dz} - \int_{s_0}^x \frac{\partial T_0}{\partial z}(x', z) dx' \right]. \quad (6.19)$$

Equation (6.19) provides us with the necessary expression to find W_0 . Clearly, in the case of zero slip $W_0 \equiv 0$ by (6.16b) and (6.17). In the case of zero friction, using (6.16a) yields

$$\frac{dW_0}{dz} = \frac{1}{s_0} \int_0^{s_0} \frac{\partial T_0}{\partial z} dx. \quad (6.20)$$

Integrating (6.19) once with respect to x using the Dirichlet condition in (6.15), we obtain

$$\Phi_0 = \left(\frac{1-2\nu}{1-\nu} \right) \left[\frac{(s_0-x)^2}{2} \frac{dW_0}{dz} - \int_x^{s_0} (x'-x) \frac{\partial T_0}{\partial z}(x', z) dx' \right]. \quad (6.21)$$

Finally, the leading-order pressure is given by

$$\begin{aligned} p_0 &= Bz - \frac{\partial \Phi_0}{\partial z}(0, z) \\ &= Bz + \left(\frac{1-2\nu}{1-\nu} \right) \frac{d}{dz} \int_0^{s_0} \left(x - \frac{s_0}{2} \right) \frac{\partial T_0}{\partial z} dx \quad (\text{zero friction}), \end{aligned} \quad (6.22a)$$

$$= Bz + \left(\frac{1-2\nu}{1-\nu} \right) \frac{d}{dz} \int_0^{s_0} x \frac{\partial T_0}{\partial z} dx \quad (\text{zero slip}). \quad (6.22b)$$

Notice that these forms of p_0 are determined solely from the thermo-elastic problem, and so are valid for any thermal distribution T_0 . Taking the zero-Stefan-number limit, we substitute the expression for T_0 from (6.11) to obtain

$$p_0 = Bz + \left(\frac{1 - 2\nu}{1 - \nu} \right) f(z), \quad (6.23)$$

where

$$f(z) = \frac{d}{dz} \left(\frac{s_0^3}{12} \frac{d^2 s_0}{dz^2} \right) \quad (\text{zero friction}), \quad (6.24a)$$

$$f(z) = -\frac{d^3}{dz^3} \left(\frac{s_0^4}{24} \right) \quad (\text{zero slip}). \quad (6.24b)$$

The two forms of $f(z)$ that we obtain, depending on whether we impose zero friction or zero slip between the metal and the mold, differ in one crucial respect, namely *the sign of the highest derivative of s_0* . Hence we may expect the behavior of the solutions that result to be quite different in the two cases. This certainly suggests that considerable care should be taken in imposing the right contact conditions on the mold: the character of the solution may be largely determined by them.

The leading-order constitutive relation is coupled to (6.23) *via* the expression for R obtained from the second equation in (6.11):

$$R(p_0) = \frac{1}{s'_0(z)} - s_0(z). \quad (6.25)$$

The functional form of $R(p)$ must be determined experimentally. For the purposes of this report we restrict our attention to the simple case in which the heat transfer coefficient $1/\tilde{R}$ is linear in the pressure, say

$$\frac{1}{\tilde{R}} = h(h_0 + h_1 \tilde{p}), \quad (6.26)$$

where h_0 and h_1 are constants. Since \tilde{R} is not constant, we have to devise a way in which the parameter h can be defined uniquely.

First, we note that we expect the heat transfer coefficient to be very small when the pressure is zero, so we expect $h_0 \ll 1$. In the special case that $h_0 = 0$, we see that for $\tilde{R}^{-1} = h$ at hydrostatic pressure as described earlier, h_1 would not be constant. Therefore, we choose to set $\tilde{R}^{-1} = h$ at hydrostatic pressure *at the characteristic depth z_c* , and thus we obtain

$$h_1 = \frac{1}{\rho g z_c}.$$

Recalling the definition of z_c , h is defined by

$$h^3 = \frac{\rho^2 g L k V}{\Delta T} \frac{d}{d\tilde{p}} \left(\frac{1}{\tilde{R}} \right).$$

Combining equations (6.25) and (6.26) while recalling that $R = h\tilde{R}$, we obtain

$$\begin{aligned} \left(\frac{1}{s'_0} - s_0\right)^{-1} &= h_0 + \frac{2\epsilon^2(\lambda + \mu)\alpha\Delta T}{\rho g z_c} p_0 \\ \frac{s'_0}{1 - s_0 s'_0} &= h_0 + \frac{1}{B} \left[Bz + \left(\frac{1 - 2\nu}{1 - \nu}\right) f(z) \right] \\ \frac{s'_0}{1 - s_0 s'_0} &= h_0 + z + \gamma f(z), \end{aligned} \quad (6.27a)$$

$$\begin{aligned} \gamma &= \frac{1}{B} \left(\frac{1 - 2\nu}{1 - \nu}\right) = \frac{x_c^2 \alpha E \Delta T}{\rho g z_c^3 (1 - \nu^2)} \\ &= \frac{E \alpha h^4 (\Delta T)^4}{\rho^4 g L^3 k V^3 (1 - \nu^2)}. \end{aligned} \quad (6.27b)$$

Note that when $\gamma = 0$, there is no temperature differential to drive thermal stresses, and hence the pressure is purely hydrostatic.

Substituting either of (6.24) into (6.27a), we obtain a single ordinary differential equation for s_0 , depending on the two parameters h_0 and γ . In the case of zero friction this reads

$$\frac{\gamma}{12} (s_0^3 s_0'')' + z + h_0 - \frac{s'_0}{1 - s_0 s'_0} = 0, \quad (6.28a)$$

while for zero slip we obtain

$$\frac{\gamma}{24} (s_0^4)''' - z - h_0 + \frac{s'_0}{1 - s_0 s'_0} = 0. \quad (6.28b)$$

As initial conditions for (6.28) we specify zero thickness and zero pressure at the entry point $z = 0$:

$$s_0(0) = 0, \quad f(0) = 0.$$

In the case of zero friction the initial behavior of s is thus

$$\begin{aligned} s_0(z) &\sim h_0 z + (1 - h_0^3) \frac{z^2}{2} + h_0^2 (-10 + \gamma h_0 + 6h_0^3 - \gamma h_0^4) \frac{z^3}{12} + \dots \\ &+ \text{const. } z^{9/4} \exp\left(-4\sqrt{\frac{3}{\gamma h_0^3 z}}\right) + \dots \quad \text{as } z \rightarrow 0. \end{aligned} \quad (6.29a)$$

The arbitrary constant multiplying the exponentially small term parametrizes a one-parameter family of solutions with the correct behavior as $z \rightarrow 0$. (Note that the contribution from this one-parameter family also becomes transcendentally small in the limit that $h_0 \rightarrow 0$.)

In contrast, in the case of zero slip if we disallow unphysical oscillatory behavior, there is just one solution satisfying the initial conditions, with

$$s_0(z) \sim h_0 z + (1 - h_0^3 - \gamma h_0^4) \frac{z^2}{2} + h_0^2 (-5 - 10\gamma h_0 + 3h_0^3 + 15\gamma h_0^4 + 10\gamma^2 h_0^5) \frac{z^3}{6} + \dots \quad (6.29b)$$

as $z \rightarrow 0$. This indicates that in the latter case we can solve (6.28b) as an initial-value problem, using (6.29b) as the initial condition. However, (6.28a) is *not* well posed as an initial-value problem: a further boundary condition (*e.g.* specifying the behavior as $z \rightarrow \infty$) is needed to determine the solution uniquely. It is not at all clear what such a condition should be, so from now on we consider only the zero-slip problem (6.28b) and (6.29b) which in any case is likely to be of more physical relevance than the zero-friction case.

As further evidence that equations (6.28b) and (6.29b) form a well-posed initial-value problem, we can verify that there are three degrees of freedom in the asymptotic behavior of the solution for large z :

$$s \sim \sqrt{2z} + \frac{A_1}{\sqrt{z}} + \frac{1}{z} - \frac{A_1^2}{(2z)^{3/2}} + \dots \\ + z^{-9/8} \left\{ A_2 \cos \left(\frac{4 \times 18^{1/4} z^{7/4}}{7\sqrt{\gamma}} \right) + A_3 \sin \left(\frac{4 \times 18^{1/4} z^{7/4}}{7\sqrt{\gamma}} \right) \right\} + \dots \quad (6.30)$$

as $z \rightarrow \infty$; A_1 , A_2 and A_3 are arbitrary constants. The oscillatory behavior of (6.30) is encouraging since significant oscillations in the free surface have been observed in experiments.

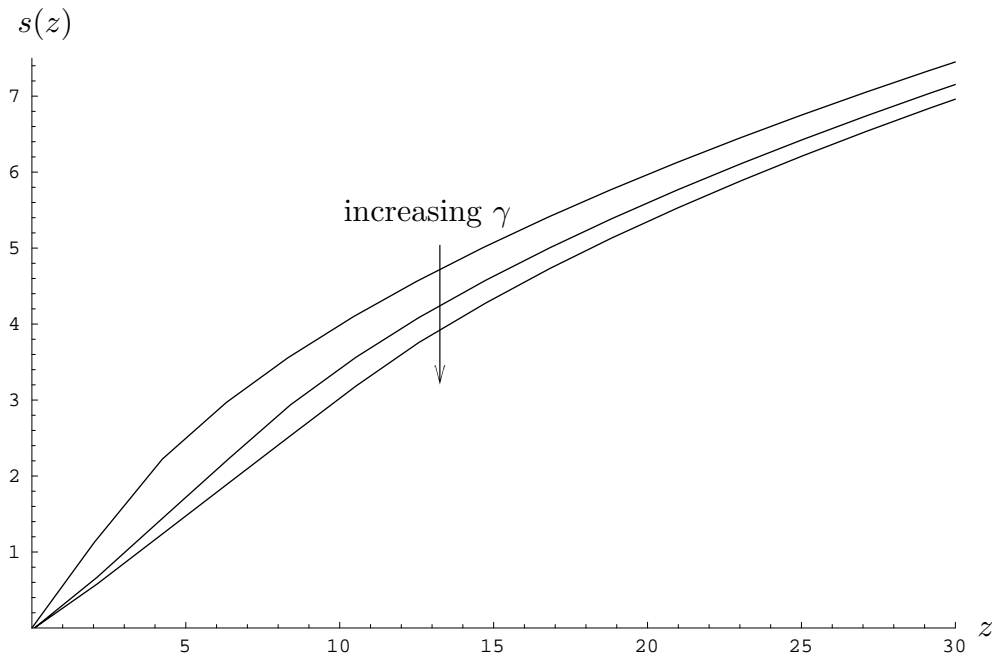


Figure 5. A numerical plot of the free boundary $s(z)$ (as governed by (6.28b)) *vs.* depth z , with parameter values $h_0 = 0$ and $\gamma = 0, 50, 100$. Here increasing γ increases the spike severity.

Finally, we now present some numerical solutions of (6.28b) and (6.29b). Since h_0 , the heat transfer at zero pressure, is expected to be rather small, we set $h_0 = 0$ and examine the effect of varying γ . As shown in Fig. 5, the free surface $s(z)$ is not greatly

affected by rather large changes in γ . In particular, the oscillatory behavior suggested by (6.30) appears to be swamped by the algebraic growth of s , and there is no evidence of large-amplitude oscillations like those reported experimentally.

However, the pressure distribution *does* vary quite dramatically as γ is increased, as shown in Fig. 6. When $\gamma = 0$, there are no thermal stresses and the pressure is purely hydrostatic. For nonzero γ , p oscillates about its hydrostatic value, the amplitude of the oscillations increasing with γ . Such behavior is consistent with the asymptotic form (6.30) of s : substitution of (6.30) into (6.23) shows that oscillations in p have growing amplitude, with

$$p \sim z + \sqrt{\frac{3}{\gamma}} 2^{5/4} z^{21/8} \left\{ A_3 \cos \left(\frac{4 \times 18^{1/4} z^{7/4}}{7\sqrt{\gamma}} \right) - A_2 \sin \left(\frac{4 \times 18^{1/4} z^{7/4}}{7\sqrt{\gamma}} \right) \right\} + \dots$$

These large variations in pressure may well be the cause of the surface instability observed in experiments.

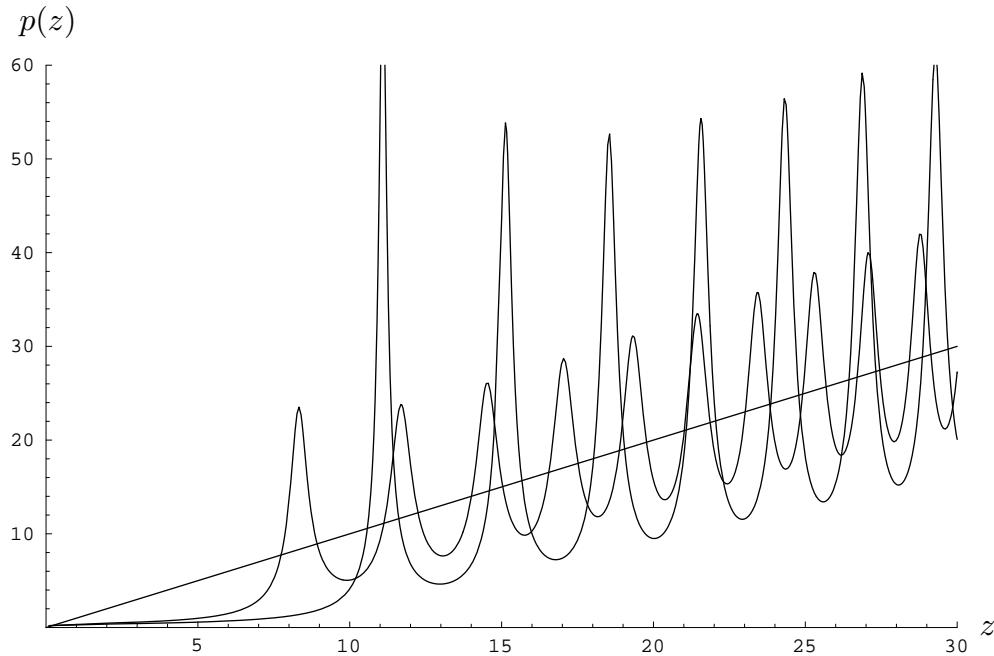


Figure 6. A numerical plot of the pressure $p(z)$ [as governed by (6.28b)] *vs.* depth z , with parameter values $h_0 = 0$ and $\gamma = 0, 50, 100$. When $\gamma = 0$, the pressure is purely hydrostatic.

Section 7: Conclusions and Further Research

A mathematical model for the initiation of air gaps between a forming mold and solidifying melt was written down and perturbation approximations were furnished in various cases where certain parameters were assumed to be small. The focus of the modeling was on examination of possible causes of surface irregularities in the solid.

The main task completed was a derivation of equations and boundary conditions for both heat conduction and elasticity effects. These two sets of equations are coupled by the contact pressure at the mold-solid interface. The coupling occurs because the contact pressure appears in a boundary condition for the temperature while it is also a component of the stress tensor. A nondimensionalization of these coupled equations and condition with a set of scales that are physically realistic was also derived.

Several asymptotic solutions of the thermal problem were found that support the \sqrt{z} shape shown in Fig. 2. These approximations were found assuming small Stefan number in one case and small z in the other. We also derived an approximation with the Megerlin method (see [2]).

To explore possible sources of surface irregularities, we considered the case where the mold's surface has oscillations. In this situation, which we referred to as the "mavy mold" case, we found that the oscillations were induced onto the solid-melt interface but were damped exponentially for large x as in Fig. 3.

Lastly we studied the full thermoelastic problem using the equations of hypo-thermoelasticity and derived asymptotic approximate solutions for the shape of the solid-liquid interface. We made a simplifying assumption that the relationship between the heat transfer coefficient on the mold-melt interface and the pressure was linear. Here, we again found our approximation had the \sqrt{z} shape for the solid. We also found oscillations present in the formula for the pressure.

Below we list some future directions for the work begun at the MPI meeting which was described in this report.

1. Examine the effects due to changes in temperature in the mold which will introduce thermal stresses. We wish to know how important these effects are and if they can be included in this model.
2. Incorporate the wavy mold solution for T and s which were found in §5 by coupling to the effects of the elastic part of the problem. This would lead to a new equation for the s function.
3. Add in the effects of the fluid motion in the molten metal. This would allow us to gain precise information on the shape of the meniscus (see Fig. 4) that forms at the surface of the molten metal where the mold enters. We would hope to see how the molten metal folds over and quantify the sizes and shapes of the air gaps (again see Fig. 4). Here we would also study the full thermoelastic problem. The presence of air gaps would lead to dramatic changes in heat transfer between the mold and the molten metal that would introduce large thermal stresses.

4. Further explore the solutions found in §6 which have oscillatory behavior. The focus here would be on determining the causes of the irregular behavior.

Appendix

For the thermal conductivity k , we have the following [5]:

$$k = 229.4 \frac{\text{J}}{\text{m} \cdot \text{s} \cdot ^\circ\text{C}}. \quad (\text{A.1})$$

For the density ρ of the mold, we have [5]

$$\rho = 2650 \frac{\text{kg}}{\text{m}^3}. \quad (\text{A.2})$$

Reference [5] gives the following value for the thermal diffusivity $\kappa = k/\rho c_p$ of the metal:

$$\kappa = 8.2 \times 10^{-5} \frac{\text{m}^2}{\text{s}}. \quad (\text{A.3})$$

For the specific heat, we don't have a specific value. Rather, we had the following quoted estimate:

$$c_p = 3 \times 10^3 \frac{\text{J}}{\text{kg} \cdot ^\circ\text{C}}.$$

However, if we use the values from (A.1)–(A.3) and the definition of κ , we have

$$c_p = \frac{k}{\rho\kappa} = 1.06 \times 10^3 \frac{\text{J}}{\text{kg} \cdot ^\circ\text{C}}, \quad (\text{A.4})$$

and it is this value we use in our analysis.

For the latent heat of melting L , we have [5]

$$L = 3.9 \times 10^5 \frac{\text{J}}{\text{kg}}. \quad (\text{A.5})$$

For the velocity V , we were quoted a range of 0–250 mm/s. Therefore, we use for a characteristic velocity the value

$$V = 10^{-1} \frac{\text{m}}{\text{s}}. \quad (\text{A.6})$$

For the temperature differential ΔT , we note that initially the mold is at room temperature, so we have

$$T_s = 25^\circ\text{C}. \quad (\text{A.7a})$$

In [5] we are given a value of

$$T_f = 660^\circ\text{C}, \quad (\text{A.7a})$$

and thus the differential is

$$\Delta T = 635^\circ\text{C}. \quad (\text{A.8})$$

Lastly we consider the heat transfer coefficient h , which may be calculated from a characteristic heat flux Q *via* the relation $h = Q/\Delta T$. In [5] we are given a value of

$$Q = 7.2 \times 10^4 \frac{\text{J}}{\text{m}^2 \cdot \text{s}},$$

but we have decided that this was for a different problem. We were also given a value of

$$h = 1100 \frac{\text{J}}{\text{m}^2 \cdot \text{s} \cdot ^\circ\text{C}},$$

but we aren't sure of the value and have discarded it. In [6], they quote a value of

$$Q = 6 \times 10^6 \frac{\text{J}}{\text{m}^2 \cdot \text{s}},$$

and so using the relation, we have that

$$h = 9.45 \times 10^3 \frac{\text{J}}{\text{m}^2 \cdot \text{s} \cdot ^\circ\text{C}}. \quad (\text{A.9})$$

For \tilde{a} , the amplitude of the undulations, we were initially given the following upper bound:

$$\tilde{a} = 10^{-5} \text{ m}, \quad (\text{A.10a})$$

but later it was revised downward to

$$\tilde{a} = 10^{-6} \text{ m}. \quad (\text{A.10b})$$

For $\tilde{\ell}$, the wavelength of the undulations, we were given the following upper bound:

$$\tilde{\ell} = 5 \times 10^{-4} \text{ m}, \quad (\text{A.11a})$$

but later it was revised downward to

$$\tilde{\ell} = 10^{-3} \text{ m}. \quad (\text{A.11b})$$

The coefficient of thermal expansion is given in [5] as

$$\alpha = \frac{37.8 \times 10^{-6}}{^\circ\text{C}}. \quad (\text{A.12})$$

In addition, the Young's modulus is given there as

$$E = 6 \times 10^{10} \frac{\text{kg}}{\text{m} \cdot \text{s}^2}, \quad (\text{A.13})$$

but as discussed in §6, we feel that this is too high for the temperature ranges under consideration.

Nomenclature

Variables and Parameters

Units are listed in terms of length (L), mass (M), moles (N), time (T), or temperature (Θ). The equation number where a particular quantity first appears is listed.

- \tilde{a} : amplitude of undulation in mold, units L (5.1).
- A : arbitrary function or constant, variously defined.
- B : ratio measuring relative effects of hydrostatic pressure and thermal stresses, value $\rho g z_c^3 / 2x_c^2(\lambda + \mu)\alpha\Delta T$ (6.5a).
- c_p : specific heat of solid, units $L^2T^{-2}\Theta^{-1}$ (2.1).
- E : Young's modulus of solid, units $ML^{-1}T^{-2}$.
- $f(z)$: function describing differential front operator for particular elastic boundary condition (6.23).
- g : acceleration due to gravity, units LT^{-2} (6.1).
- h : heat transfer coefficient at hydrostatic pressure, units $MT^{-3}\Theta^{-1}$ (2.5b).
- k : thermal conductivity of solid, units $ML\Theta^{-1}T^{-3}$ (2.1).
- $\tilde{\ell}$: wavelength of undulation in mold, units L (5.1).
- L : latent heat of fusion, units L^2T^{-2} (2.4).
- $\tilde{p}(\tilde{z})$: thermal contact pressure, units $ML^{-1}T^{-2}$.
- Q : heat flux, units MT^{-3} .
- \tilde{R} : thermal contact resistance, units $\Theta T^3 M^{-1}$ (2.2).
- $S(\zeta, \tau)$: front position near tip (5.21a).
- $\tilde{s}(\tilde{z}, t)$: freezing front, units L .
- St : Stefan number, value $c_p\Delta T/L$.
- \tilde{t} : time from beginning of experiment, units T .
- $\tilde{T}(\tilde{x}, \tilde{z}, \tilde{t})$: temperature, units Θ (2.1).
- $U(x, z)$: steady "velocity" in the x -direction (6.13a).
- $\tilde{u}(\tilde{x}, \tilde{z})$: displacement in the \tilde{x} -direction, units L (6.3a).
- V : velocity of mold, units LT^{-1} (2.1).
- $W(x, z)$: steady "velocity" in the z -direction (6.13b).
- $\tilde{w}(\tilde{x}, \tilde{z})$: displacement in the \tilde{z} -direction, units L (6.3a).
- \tilde{x} : distance measured normal to the surface of the mold, units L .
- \mathcal{Z} : the integers.
- \tilde{z} : distance measured parallel to the surface of the mold, units L .
- α : coefficient of thermal expansion, units Θ^{-1} (6.3a).
- γ : constant, value $E\alpha h^4(\Delta T)^4/\rho^4 g L^3 k V^3(1 - \nu^2)$ (6.27a).
- ϵ : ratio of characteristic \tilde{x} length scale to characteristic \tilde{z} length scale, value $h\Delta T/\rho LV$.
- ζ : scaled z -coordinate near tip (5.21a).

- η : fast oscillation scale in undulation case, value $(z - t)/\epsilon$.
 $\theta(\xi, \zeta, \tau)$: temperature near tip (5.21a).
 κ : thermal diffusivity, value $k/\rho c_p$, units $L^2 T^{-1}$ (A.3).
 λ : Lamé constant, units $ML^{-1} T^{-2}$ (6.3a).
 μ : Lamé constant, units $ML^{-1} T^{-2}$ (6.3a).
 ν : Poisson's ration (6.5a).
 ξ : scaled x -coordinate near tip (5.21a).
 ρ : density of solid, units ML^{-3} (2.1).
 $\tilde{\sigma}(\tilde{x}, \tilde{z})$: stress tensor, units $ML^{-1} T^{-2}$ (6.1a).
 τ : scaled t -coordinate near tip (5.21a).
 $\Phi(x, z)$: reduced Airy stress function (6.13a).
 $\tilde{\phi}(\tilde{x}, \tilde{z})$: displacement Airy stress function, units MLT^{-2} (6.2).

Other Notation

- c : as a subscript, used to indicate a characteristic value.
 f : as a subscript, used to indicate freezing.
 flat : as a subscript, used to indicate the flat mold (5.13a).
 I : as a subscript, used to refer to the integral method (4.11).
 ℓ : as a subscript, used to indicate the ℓ scaling (5.21a).
 M : as a subscript, used to refer to the Megerlin method (4.5).
 m : as a subscript, used to refer to the undulating mold (5.13a).
 s : as a subscript, used to indicate a quantity on the mold.
 \tilde{x} : as a subscript, used to indicate the \tilde{x} -component of stress (6.1).
 \tilde{z} : as a subscript, used to indicate the \tilde{z} -component of stress (6.1).
 Δ : refers to a differential in temperature (2.5a).
 $n \in \mathcal{Z}$: as a subscript, used to refer to an expansion in St (3.2), \tilde{p} (6.26), or z (6.30).

References

- [1] Hector, Jr., L. G., Howarth, J. A., Kim, W.-S., Barber, J. R., and Richmond, O. “Estimation of Gap Nucleation Time During the Early Stages of Solidification on a Sinusoidal Mold Surface.” In preparation.
- [2] Alexiades, V. and Solomon, A. D. *Mathematical Modeling of Melting and Freezing Processes*. Washington: Hemisphere, 1993.
- [3] Kevorkian, J. and Cole, J. D. *Perturbation Methods in Applied Mathematics*. New York: Springer Verlag, 1981.
- [4] Nishida, Y., and Matsubara, H. “Effect of Pressure on Heat Transfer at the Metal Mould-Casting Interface.” *Brit. Found.* **69**, pp. 274–78 (1976).
- [5] Richmond, O., Hector, Jr., L. G., and Fridy, J. “Growth Instability During Nonuniform Directional Solidification of Pure Metals.” *J. Appl. Mech.* **57**, pp. 529–536 (1990).
- [6] Ackermann, P., Heinemann, W., and Kurz, W. “Surface Quality and Meniscus Solidification in Pure Chill Cast Metals.” *Arch. Eisen.* **55**, pp. 1–8 (1984).

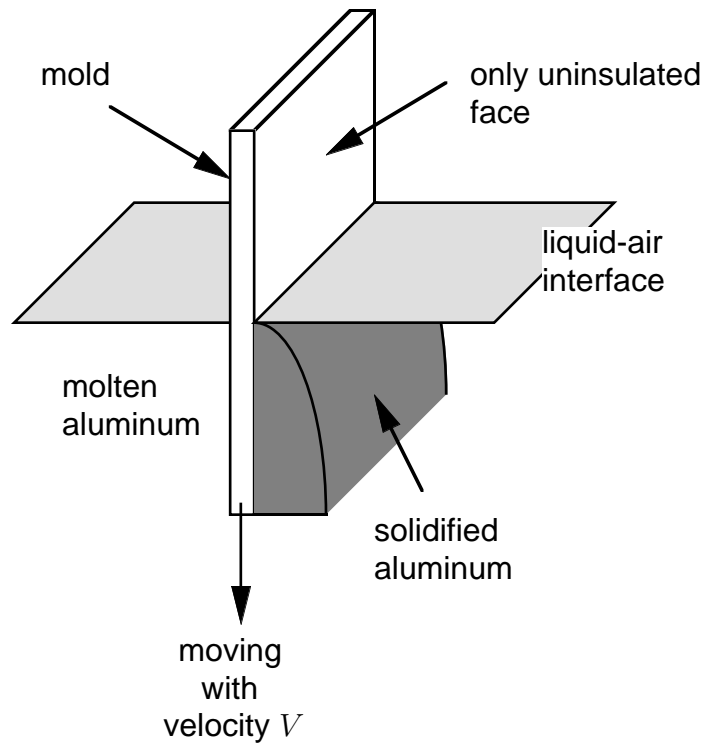


Figure 1. Schematic representation of problem.

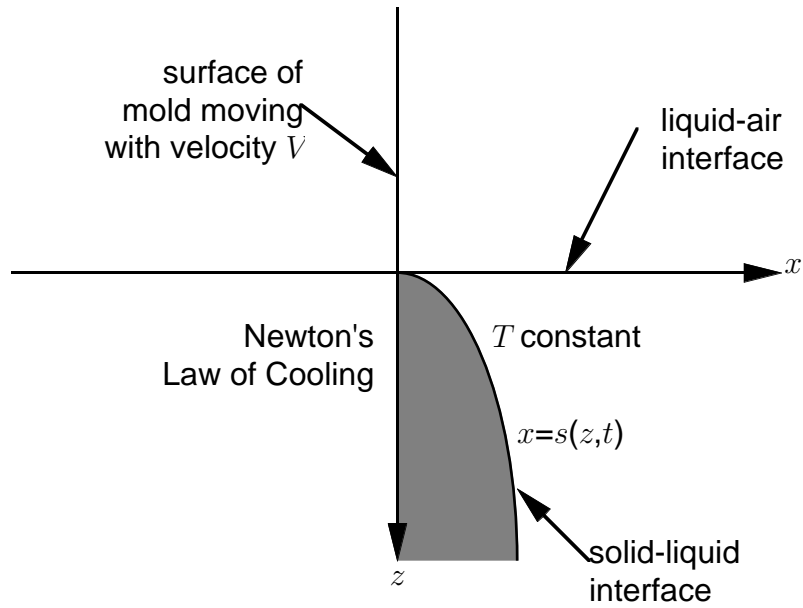


Figure 2. Mathematical representation of problem.

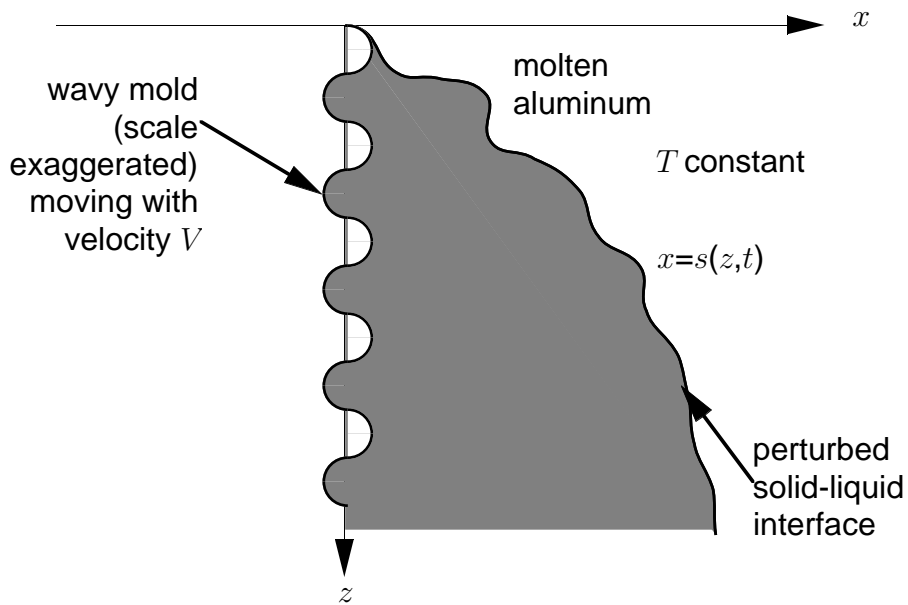


Figure 3. Undulating mold problem.

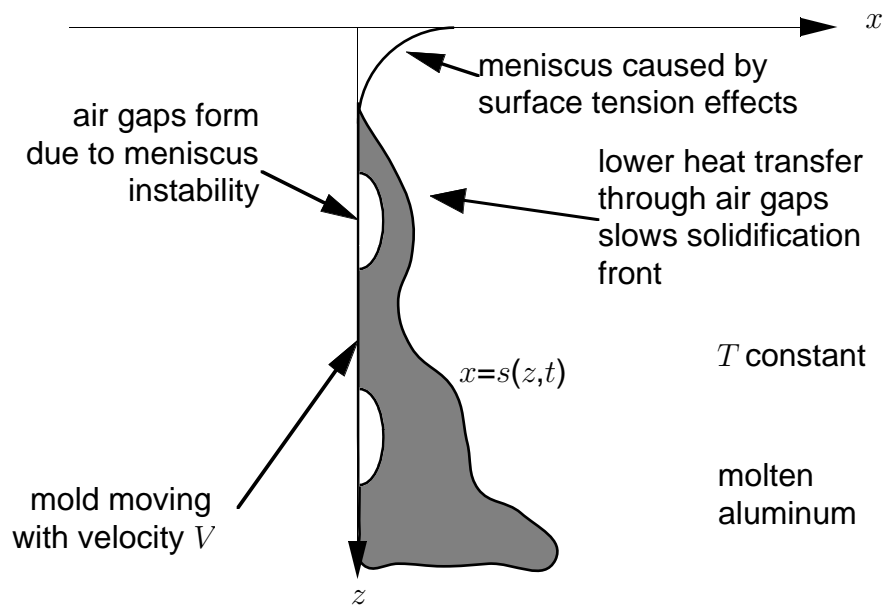


Figure 4. Meniscus/air gap problem.